

CLIMATE CHANGE

26/2024

Final report

Testing of a verification scheme for integrating non-CO₂ aviation effects into EU ETS

by:

Malte Niklaß, Alexander Lau
DLR Institute of Air Transport, Hamburg

Katrin Dahlmann
DLR Institute of Atmospheric Physics, Oberpfaffenhofen

Martin Plohr
DLR Institute of Propulsion Technology, Cologne

publisher:

German Environment Agency

CLIMATE CHANGE 26/2024

Ressortforschungsplan of the Federal Ministry for the Environment, Nature Conservation, Nuclear Safety and Consumer Protection

Project No. (FKZ) 3720 42 502 0

FB001291/ENG

Final report

Testing of a verification scheme for integrating non-CO₂ aviation effects into EU ETS

by

Malte Niklaß, Alexander Lau

DLR Institute of Air Transport, Hamburg

Katrin Dahlmann

DLR Institute of Atmospheric Physics, Oberpfaffenhofen

Martin Plohr

DLR Institute of Propulsion Technology, Cologne

On behalf of the German Environment Agency

Imprint

Publisher

Umweltbundesamt
Wörlitzer Platz 1
06844 Dessau-Roßlau
Tel: +49 340-2103-0
Fax: +49 340-2103-2285
buergerservice@uba.de
Internet: www.umweltbundesamt.de

Report performed by:

Deutsches Zentrum für Luft- und Raumfahrt (DLR)
Linder Höhe
51147 Cologne
Country

Report completed in:

July 2023

Edited by:

Section V 3.6 Aviation
Kay Köhler

Publication as pdf:

<http://www.umweltbundesamt.de/publikationen>

ISSN 1862-4359

Dessau-Roßlau, July 2024

The responsibility for the content of this publication lies with the author(s).

Abstract: Testing of a verification scheme for integrating non-CO₂ aviation effects into EU ETS

In order to achieve a reduction in non-CO₂ effects, the European Parliament (EP) voted on June 8, 2022 to expand the scope of the EU Emissions Trading System (EU ETS) (EP, 2022). In December 2022 the European Council, the European Commission (EC) and the EP reached an agreement on the revision of the EU ETS. According to the agreement, non-CO₂ effects can no longer be ignored and the EC should set up a monitoring, reporting and verification (MRV) scheme for non-CO₂ aviation emissions from 2025, as a first step for the full integration of non-CO₂ effects into the EU ETS. This project focuses on the development and testing of such an MRV system. For this purpose, non-CO₂ effects are integrated according to the principle of equivalent CO₂ emissions (CO₂e). Since several CO₂e calculation methods are basically available, the process of selection involves a trade-off between the level of atmospheric uncertainties, the level of climate mitigation incentives, and the resulting effort of MRV activities (see Section 1.2).

In the present report we take over the perspective of an agency and analyze all necessary tasks for the verification of reported location-dependent CO₂ equivalents (Input of Task 1). To reduce the additional MRV effort to a minimum, all necessary CO₂e validation steps should automatically be performed by a standardized CO₂e software, possibly provided directly by the EC or by an approved organization. This includes the query and processing of 4-D flight profile data from an independent data source, the verification of the reported CO₂ (fuel burn), the estimation of fuel flow and non-CO₂ emissions along the flight path, and the estimation of equivalent CO₂ emissions per flight. Analogous to the CO₂ monitoring in EU ETS and under CORSIA, different computation methods can be made available for the physical-based modules. The selection of the calculation methods used by an individual aircraft operator should be specified in the airline specific Emission Monitoring Plan (EMP) and submitted to the competent authority for approval. The allocation of the level of CO₂e surrender obligations is a political decision and not part of this project.

Kurzbeschreibung: Erprobung eines Verifizierungssystems für Nicht-CO₂-Effekte des Luftverkehrs

Mit dem Ziel die Klimawirkung des Luftverkehrs zu reduzieren, votierte das Europäische Parlament (EP) am 8. Juni 2022 dafür, das EU-Emissionshandelssystem (EU ETS) um Nicht-CO₂-Effekte zu erweitern (EP, 2022). Im Dezember 2022 einigten sich der Europäische Rat, die Europäische Kommission (KOM) und das EP auf eine entsprechende Änderung des EU ETS. Gemäß des Gesetzesänderungsbeschlusses dürfen Nicht-CO₂-Effekte nicht länger ignoriert werden und sollen, als erster Schritt zur vollständigen Integration in das EU-ETS, ab 2025 durch ein von der KOM entworfenes Überwachungs-, Berichterstattungs- und Verifizierungssystem (MRV) erfasst werden. Dieses Projekt behandelt die Entwicklung und Erprobung eines solchen Systems. Die Nicht-CO₂-Effekte werden dabei nach dem Prinzip der CO₂-Äquivalente (CO₂e) erfasst. Da verschiedene Ansätze zur Berechnung von CO₂e zur Verfügung stehen, muss bei der Wahl der Berechnungsmethode eine Abwägung zwischen möglichst geringen atmosphärischen Unsicherheiten, möglichst hohen Klimaschutzanreizen und möglichst geringem Aufwand für MRV-Aktivitäten gefunden werden (siehe Abschnitt 1.2).

In diesem Bericht analysieren wir aus der Perspektive einer Emissionshandelsstelle alle notwendigen Aufgaben zur Verifizierung der berichteten ortsabhängigen CO₂-Äquivalenten (Input aus AP 1). Um dabei den zusätzlichen MRV-Aufwand auf ein Minimum zu reduzieren, sollten alle notwendigen CO₂e-Validierungsschritte automatisch von einer standardisierten CO₂e-Software durchgeführt werden, die direkt von der KOM oder einer zugelassenen Organisation bereitgestellt wird. Dies umfasst die Abfrage und Verarbeitung von 4-D-Flugprofildaten aus einer unabhängigen Datenquelle, die Verifizierung der berichteten CO₂-Emissionen (Treibstoffverbrauch), die Abschätzung des Kraftstoffdurchsatzes und der Nicht-

CO₂-Emissionen entlang des Flugprofils sowie die Berechnung der CO₂-Äquivalente pro Flug. Analog zum CO₂-Monitoring im EU ETS und unter CORSIA können für die physikalisch basierten Module unterschiedliche Berechnungsverfahren zur Verfügung gestellt werden. Die Auswahl der verwendeten Berechnungsmethoden gilt es im Emissionsüberwachungsplan (EMP) durch den Betreiber festzulegen, welcher der zuständigen Behörde zur Genehmigung vorgelegt wird. Die Bestimmung einer expliziten Höhe der CO2e-Abgabepflicht ist eine politische Entscheidung und wurde nicht im Projekt untersucht.

Table of content

List of figures	8
List of tables	8
List of abbreviations	10
1 Introduction.....	11
1.1 Short overview of climate effects of aviation and possible mitigation approaches.....	11
1.2 Options for integrating non-CO ₂ effects of aviation into EU ETS and under CORSIA	11
1.3 Integration into the project	13
2 Verification software for CO ₂ equivalents per flight	15
2.1 Minimum data to be reported to the authority	16
2.2 Query and processing of flight plan data.....	19
2.3 Fuel burn module: Verification of the reported CO ₂ and simplified Fuel Flow estimation ..	21
2.3.1 Application of aircraft specific regression formulas	21
2.3.2 Application of aircraft and distance specific 3-D fuel profiles.....	24
2.3.3 Detailed trajectory simulations taking wind effects into account.....	27
2.4 Emission module: Evaluation of non-CO ₂ emissions per flight	28
2.4.1 Evaluation of CO ₂ and H ₂ O Emissions	28
2.4.2 Evaluation of NO _x Emissions	28
2.4.3 Application of methodology for estimated Fuel Flow data	30
2.4.4 Uncertainties of NO _x prediction.....	31
2.5 Climate-response module: Evaluation of CO ₂ equivalents per flight.....	31
3 Comparison of CO2e with results of DLR simplified CO2e estimator (Task 3).....	34
3.1 Emissions.....	34
3.2 Climate impact	35
4 Summary	38
5 List of references	40

List of figures

Figure 1:	Mitigation benefit and effort for monitoring, reporting and verification (MRV) activities of different CO ₂ e calculation methods.....	12
Figure 2:	Overview of current project activities	13
Figure 3:	Monitoring and reporting steps for integrating non-CO ₂ aviation effects into EU ETS (Niklaß et al., 2022, p. 13)	14
Figure 4:	Possible structure of the required software for CO ₂ e verifications per flight.....	15
Figure 5:	Exemplary comparison of the last filed flight plan (model 1 data, red), the recorded flight path (model 3 data, blue) and the flight monitoring data of the airline (green) of a single flight	20
Figure 6:	Possible logic of the fuel burn module	21
Figure 7:	Relative fuel share per flight phase as a function of the flight distance	23
Figure 8:	Identification of Top of Climb (ToC) and Top of Descent (ToD) to determine flight time during climb, cruise and descent.....	23
Figure 9:	Vertical mission profile of reduced emission profiles (REP).....	25
Figure 10:	Example of EI NO _x data calculated for a flight data recording with the Boeing Fuel Flow method	30
Figure 11:	Altitude profile for the route ATH-LCA.....	35
Figure 12:	Relative deviation of the CO ₂ e calculated with the DLR simplified CO ₂ e estimator and AirClim calculations (logarithmic scale).....	37

List of tables

Table 1:	Overview of the properties of various CO ₂ e calculation methods (Niklaß et al., 2022, p. 14), gray text indicates information that is identical to simpler calculation methodologies.....	17
Table 2:	Possible EU ETS report of non-CO ₂ effects per flights	19
Table 3:	Relative deviation (in %) between the airline's flight monitoring data and the DDR m3 flight profile data requested by EUROCONTROL.....	20
Table 4:	Relative deviation (in %) between reported block fuel data and fuel consumption estimated with regression formulas	22
Table 5:	Relative deviation (in %) between monitored and estimated times and distances during climb, cruise and descent for all aircraft types.....	24

Table 6:	Relative deviation (in %) between monitored fuel burn and fuel burn estimated with regression formulas during climb, cruise and descent	24
Table 7:	Relative deviation (in %) between reported block fuel data and fuel consumption estimated with 3-D fuel profiles and regression formulas (brackets).....	26
Table 8:	Relative deviation (in %) between reported block fuel data and fuel consumption estimated with detailed trajectory simulations and 3-D fuel profiles [square brackets].....	27
Table 9:	Relative deviation (in %) between NO _x emissions evaluated with monitored (Task1) and estimated (Task 2) Fuel Flow data. Results are shown for FF estimation based on regression formulas and detailed trajectory simulations (brackets)	30
Table 10:	Relative deviation (in %) between CO2e emissions evaluated with monitored (Task 1) and estimated (Task 2) Fuel Flow data. Results are shown for FF estimation based on regression formulas and detailed trajectory simulations (brackets)	32
Table 11:	Assignment of aircraft data to seat categories	34
Table 12:	Relative deviation (in %) between fuel, NO _x emissions and flown distances evaluated with monitored (Task 1) trajectories and the DLR simplified CO2e estimator.	34
Table 13:	Relative deviation (in %) between CO2e emissions evaluated with monitored (Task) Fuel Flow data and the simplified CO2e estimator.	35
Table 14:	CO2e calculated with reported trajectories (Task 1, EAT) and WeCare trajectories (used for regression formulas) and relative deviation of WeCare to EAT.	36
Table 15:	CO2e calculated with WeCare trajectories and results from DLR CO ₂ estimator normalized to WeCare fuel consumption and relative deviation of DLR CO ₂ estimator and WeCare	36

List of abbreviations

Abbreviation	Explanation
ATR	Averaged Temperature Response
BF	Burnt Fuel
BFFM	Boeing Fuel Flow Method
CiC	Contrail induced Cloudiness
CH₄	Methane
CO₂	Carbon Dioxide
CO2e	Carbon Dioxide Equivalent
CORSIA	Carbon Offsetting and Reduction Scheme for International Aviation
EAT	European Air Transportation Leipzig
EC	European Commission
ECMWF	European Centre for Medium-Range Weather Forecasts
EDB	ICAO Engine Exhaust Emissions Database
EF	Emission Factor
ERF	Effective Radiative Forcing
EU-ETS	EU Emissions Trading System
ETS SF	ETS Support Facility
GTP	Global Temperature Potential
GWP	Global Warming Potential
H₂O	Water Vapor
ICAO	International Civil Aviation Organization
ISSR	Ice-Supersaturated Region
MBM	Market-based Measure
MRV	Monitoring, Reporting, and Verification
NO_x	Nitrogen Oxides
O₃	Ozone
PMO	Primary Mode Ozone
REP	Reduced Emission Profile
RF	Radiative Forcing
SAC	Schmidt-Appleman Criterion
SAF	Sustainable Aviation Fuel
TAS	True Air Speed

1 Introduction

1.1 Short overview of climate effects of aviation and possible mitigation approaches

The climate change gets more and more noticeable. Since 1980, global aviation has doubled all 15 years in terms of revenue passenger kilometers with an average growth rate of about 5% per year and is expected to grow significantly in the next decades (e.g., ICAO, 2013). As aviation is one of the fastest growing sectors, the share in global CO₂ emission could rise from currently about 2% up to even 22% in 2050 (Cames et al., 2015).

Beside CO₂ emissions, also non-CO₂ emissions contribute to aviation induced climate change. Especially the impact of contrail cirrus and the effect of NO_x emissions on the concentration of ozone increases the climate impact of aviation. The impact of non-CO₂ effects of the historical emissions of aviation caused about two third of the total aviation impact in 2020 (Lee et al., 2021). However, due to strong non-linearities coupled with these effects, their impact on individual flights varies over a wide range.

There are different options to mitigate the climate impact of aviation. Besides reducing the number of flights, the climate impact can also be reduced by technical measures, alternative fuels or operational measures. Technical measures include reduction of specific fuel consumption, reduced weight and optimized aerodynamics. In addition, optimized aircraft design for flying at lower altitudes or in a broader altitude band could reduce offsets of flying climate optimized. The climate impact can also be reduced by using alternative fuels like sustainable aviation fuel (SAF) or liquid hydrogen. This does not only reduce the impact of CO₂ (as it is climate neutral if the fuel is produced with renewable energy), but has also an impact on non-CO₂ effects, e.g. contrails. Efficient flight guidance can reduce the fuel consumption and the impact on climate. As the climate impact of non-CO₂ emissions depends not only on the amount, but also on the location and time of emission, it is possible to reduce their climate impact if climate sensitive atmospheric regions are avoided (climate optimized flights).

Measures to reduce the climate impact of non-CO₂ effects often come along with an increase of cash operating costs. As operators of aircraft have little motivation to pay these additional costs voluntarily, incentives for reducing the climate impact of non-CO₂ effects can support the introduction of such measures. Including also non-CO₂ effects in emission trading schemes or marked based measures (MBM) could be a significant incentive and therefore contribution to the agreed climate goals of Paris.

1.2 Options for integrating non-CO₂ effects of aviation into EU ETS and under CORSIA

Carbon dioxide equivalents (CO₂e or CO₂eq or CO₂-e) are a common metric for unitizing the climate impact of various climate agents. Since the climate impact of CO₂ is well understood due to its independence of emission source and location, it is reasonable to express the impacts of non-CO₂ effects in relation to the impacts of CO₂. For a given type and amount of a climate agent *i*, resulting CO₂e cause the same climate response (e.g. RF or ΔT) over a specific time horizon (e.g. 20, 50 or 100 years) as CO₂:

$$\text{CO}_2\text{e}_{\text{agent } i} = \frac{\text{Climate Impact}_{\text{agent } i}}{\text{Climate Impact}_{1 \text{ kg CO}_2}}$$

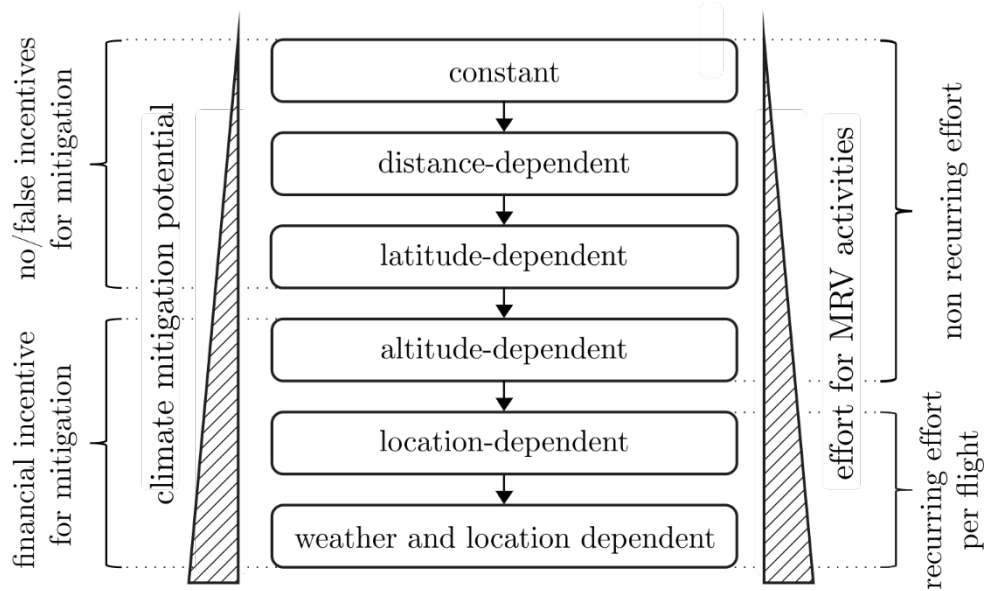
$$\text{CO2e}_{\text{total}} = \text{CO}_2 + \sum_i \text{CO2e}_{\text{agent } i}$$

In principle, there are several CO2e calculation methods available (see Figure 1) that are designed for different applications and differ, among other things, in the accuracy of the climate assessment. As a general rule, CO₂ equivalents should be easily calculable, predictable and transparent. The higher the accuracy of relevant atmospheric processes, the greater the incentives for climate mitigation. But, however, more accurate CO2e approaches will also require a higher amount of data for monitoring, reporting and verification. The selection of a CO2e calculation method is therefore a trade-off between high climate mitigation potentials and low efforts for MRV activities:

Key criteria for choosing a CO2e method:

- ▶ CO2e factors must provide incentives for actually reducing non-CO₂ effects (not simply adding costs, but providing the possibility to reduce climate impact and cost of operation)
- ▶ CO2e factors should be easily calculable, predictable and transparent

Figure 1: Mitigation benefit and effort for monitoring, reporting and verification (MRV) activities of different CO2e calculation methods



© Niklaß et al., 2020, p. 43 (adapted)

If only a constant factor is used, this increases the focus on CO₂ emissions as CO₂ emissions get more expensive. As the climate impact of non-CO₂ effects is not only dependent on the total emission strength, but also of the emission location (longitude, latitude and altitude) this might create false incentives. As an example, flying in higher altitudes decreases fuel consumption due to reduced drag, but increases the total climate impact as especially the impact of contrail cirrus and NO_x induced ozone changes increases (Matthes et al., 2021). Flying climate optimized would therefore in this case be penalized instead of rewarded with a constant CO2e factor.

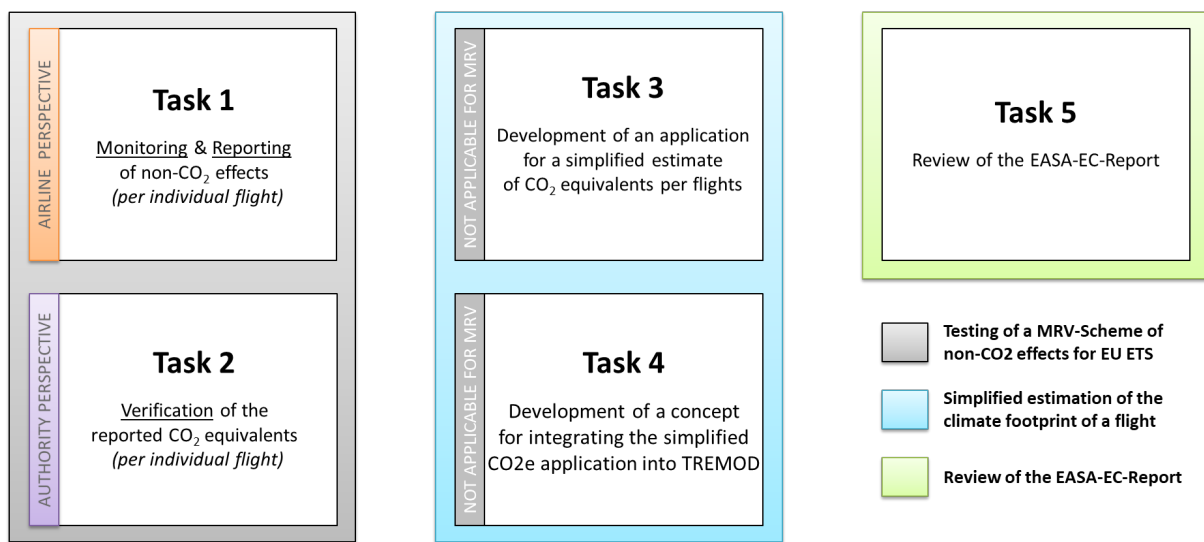
In order to avoid these misguiding incentives at least the altitude dependency of non-CO₂ effects has to be considered in the CO2e calculation method (Faber et al., 2008; Niklaß et al., 2020; Scheelhaase et al., 2016). This requires at least detailed information about the flown aircraft trajectory (altitude profile) of each flight.

Even more climate mitigation potential is received using location or even weather and location dependent factors. In this study we analyze the feasibility of using location dependent CO₂ factors. Nevertheless, simplified tools could be used to calculate estimates of the climate impact of non-CO₂ effects as a first validation or to calculate the CO₂e if the airlines are not able to provide the data. Therefore, the CO₂e estimates must be assumed conservatively to ensure, that the airlines are better off with provided data.

1.3 Integration into the project

The integration of non-CO₂ aviation effects into EU ETS will involve adjustments to the monitoring, reporting and verification procedure. This project focuses on the development and testing of an extended MRV system. Monitoring and reporting steps have been analyzed in Task 1 (see Plohr et al., 2023). The present report addresses Task 2, in which we take over the perspective of an agency and analyze all necessary tasks for verifying of reported CO₂ equivalents (Input from Task 1). Task 3 is about developing an application for a simplified estimate of CO₂ equivalents per flights (see Dahlmann et al., 2023). Since non-CO₂ climate effects are estimated here without detailed information about the actual flight route, the level of emissions and the current weather situation, this method is suitable for ecological footprint assessments and offset markets but not for emission trading. The comparison of the calculated CO₂e values for all three approaches (Task 1 to 3) is carried out in Section 3 of the present study.

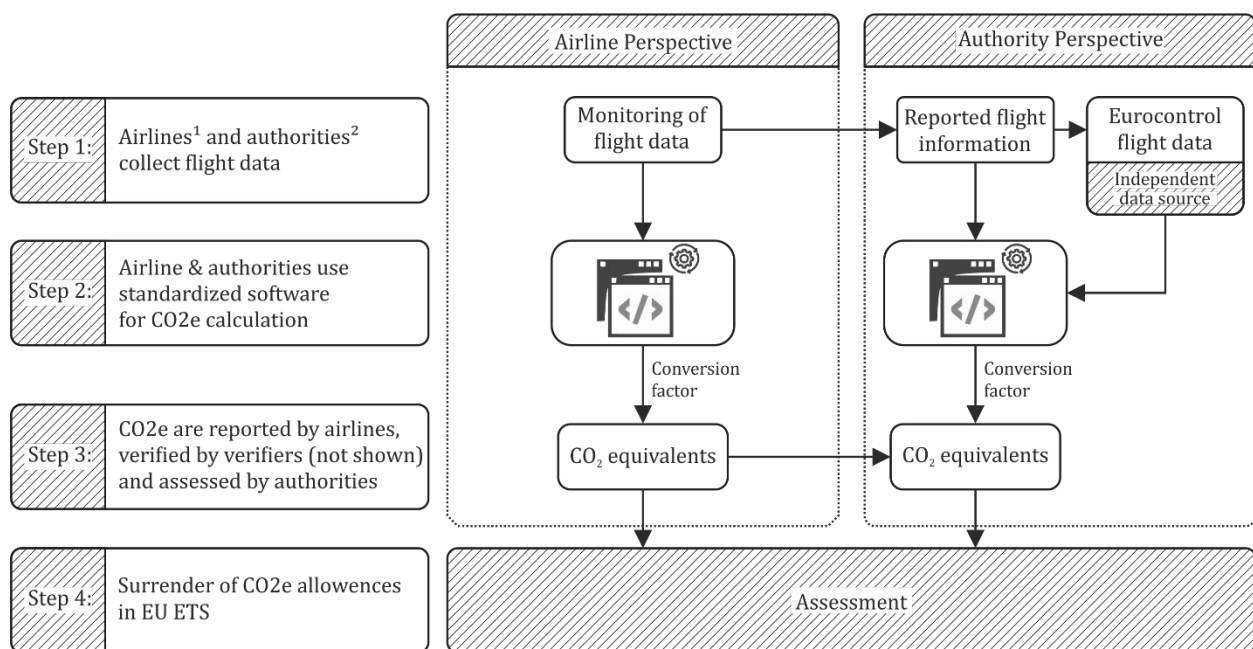
Figure 2: Overview of current project activities



© DLR

For reducing the MRV effort of non-CO₂ effects in EU ETS, we suggest to use a standardized CO₂e software (see step 2 in Figure 3 and Section 2), which might be provided or approved by the European commission (EC) for airlines (monitoring and reporting) as well as verifiers and authorities (verification and assessment). In this regard, the current EU ETS system serves as a blueprint, for which EUROCONTROL provides a web application called ETS Support Facility (ETS SF) for operators and agencies (EUROCONTROL, 2022).

Figure 3: Monitoring and reporting steps for integrating non-CO₂ aviation effects into EU ETS
(Niklaß et al., 2022, p. 13)



¹ Airlines collect flight data for all flights

² Authorities collect/request flight data for reported flights that should be assessed

© Niklaß et al., 2022, p. 13

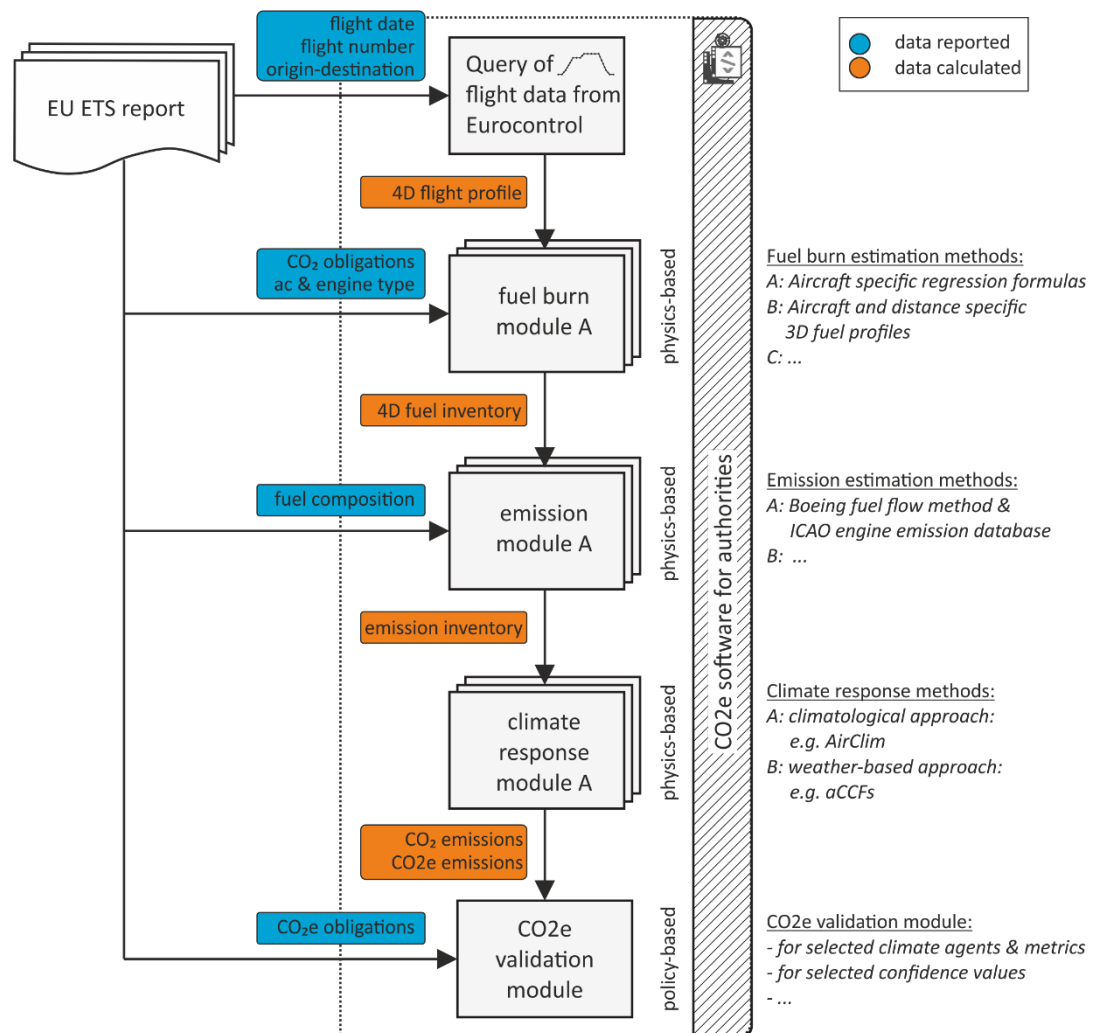
All tests of monitoring, reporting (Plohr et al., 2023), and verification procedures (present report) are based on flight data records provided by the German cargo airline European Air Transport Leipzig GmbH (EAT). EAT has agreed to support this project with data records from selected short and medium/long haul flights, most of them within Europe. In total, EAT provided data records from 449 flights on routes between 24 city pairs, covering 3 weeks in 2021 and 4 weeks in 2022. These flights were performed by 35 different aircraft identified by their individual registration. Of these aircraft 21 were Airbus A300-600s, 3 A330-200, 2 A330-300 and 9 Boeing B757-200. Selected routes cover large parts of the European airspace controlled by EUROCONTROL and represent typical flight distances within Europe. 418 domestic European flights have been supplemented by 31 intercontinental flights to the east coast of North America (Cincinnati/Northern Kentucky International Airport (CVG), Kentucky, USA; John F. Kennedy International Airport (JFK), New York, USA; Miami International Airport (MIA), Florida, USA) and to Lagos, Nigeria (Murtala Muhammed International Airport, LOS), which have been selected exemplarily for comparative purposes.

2 Verification software for CO₂ equivalents per flight

In order to reduce the additional MRV effort to a minimum, all necessary CO₂e validation steps should automatically be performed by a standardized CO₂e software (see step 2 in Figure 3 and Figure 4), possibly provided directly by the EC or by an approved organization. For the verification of location-dependent CO₂ equivalents, the standardized CO₂e software should perform following steps:

1. the query and processing of flight profile data from an independent data source like EUROCONTROL (see Section 2.2),
2. the verification of the reported CO₂ (fuel burn) and a simplified estimate of Fuel Flow along the recorded flight path (see fuel burn module in Section 2.3),
3. the computation of emission inventories for CO₂, H₂O and NO_x along the flight path (see emission module in Section 2.4), and
4. the CO₂e estimation of the flight for H₂O, NO_x, CiC under consideration of uncertainties (e.g. 5% percentile, 50% percentile, 95% percentile) for different climate indicators (e.g. ATR, GWP) and time horizons (e.g. 20, 50, 100 years) (see climate response module in Section 2.5).

Figure 4: Possible structure of the required software for CO₂e verifications per flight



Following the physical-based modules, the EU decision is implemented in a policy-based module in order to set the level of CO₂e surrender obligations (e.g., depending on the confidence levels of each climate agent):

5. Allocation of CO₂e surrender obligations (policy-based module, not part of this project)

Analogous to the CO₂ monitoring in EU ETS and under CORSIA, different computation methods can be made available for the three physical-based modules (fuel burn module, emission module and climate response module). The selection of the calculation methods used by an individual aircraft operator should be specified in the airline specific Emission Monitoring Plan (EMP) and submitted to the competent authority for approval.

To better understand the impact of uncertainties on the calculation of non-CO₂ effects and thereby on the potential of setting wrong incentives, risk assessments are required for selected climate agents. First, the climate mitigation potentials of specific strategies have to be verified. Second, reported CO₂e values have to represent estimated climate impact of aviation on average. This requires a solid data base, including flight information, fuel consumption as well as CO₂ equivalents from numerous flights. Necessary data could be collected in the pilot non-CO₂ MRV scheme of the EU ETS starting in 2025, in which non-CO₂ effects are already monitored and reported, but are not yet subject to monetary internalization.

2.1 Minimum data to be reported to the authority

The minimum data to be reported to the authority is strongly depending on the chosen CO₂e calculation method (see Figure 1 and Table 1). The higher the accuracy of relevant atmospheric processes, the greater the incentives for climate mitigation. But, however, more accurate CO₂e approaches will also require a higher amount of data for monitoring, reporting and verification. As a good compromise between high mitigation incentives of non-CO₂ impacts and reduced MRV effort (no ECMWF data required), we selected a location-dependent CO₂e factor within this work.

Table 1: Overview of the properties of various CO₂e calculation methods (Niklaß et al., 2022, p. 14), gray text indicates data/information that is identical to simpler calculation methodologies

CO ₂ e calculation method	Data to be monitored	Data to be reported	Additional MRV effort	Accuracy in climate assessment	Mitigation incentive	Possible applications
Constant	Fuel consumption	Origin-Destination Frequency Fuel consumption CO ₂ equivalents	To be neglected	very low	non	ecological footprint assessments
Distance-dependent	Fuel consumption	Origin-Destination Frequency Fuel consumption CO ₂ equivalents	To be neglected	Low	non	ecological footprint assessments
Latitude-dependent	Fuel consumption	Origin-Destination Frequency Fuel consumption CO ₂ equivalents	Standardized software needed	realistic representation on a yearly basis	non	compensation market
Altitude-dependent	Fuel consumption 3-D position Fuel flow Aircraft mass (optional) Ambient temperature	Origin-Destination Aircraft & Engine type Flight number Fuel consumption CO ₂ equivalents Take-off mass (opt.)	Standardized software needed	realistic representation on a yearly basis	Low to medium	compensation market, emission trading
Location-dependent	Fuel consumption Aircraft mass (optional) 3-D position Fuel flow Ambient temperature Ambient humidity (opt.)	Origin-Destination Aircraft & Engine type Flight number Fuel consumption CO ₂ equivalents Take-off mass (opt.)	Standardized software needed	Best estimate on a seasonal or yearly basis	Medium	emission trading

CO2e calculation method	Data to be monitored	Data to be reported	Additional MRV effort	Accuracy in climate assessment	Mitigation incentive	Possible applications
Location- & weather-dependent	Fuel consumption 4-D position Fuel flow Aircraft mass (optional) Ambient temperature Weather forecast data	Origin-Destination Aircraft & Engine type Flight number Fuel consumption CO ₂ equivalents Take-off mass (opt.)	Standardized software needed	Best estimate on a daily basis	High	emission trading

© DLR: Niklaß, Dahlmann, Maertens, Plohr and Grawe

For integrating location-dependent CO₂e factors into the EU-ETS, the minimum data to be reported to the authority are the flight date and flight number, the origin and destination airports as well as the fuel (CO₂) consumption per flight. For considering non-CO₂ climate effects, additional to this data the exact aircraft and engine type as well as the CO₂ equivalents due to the non-CO₂ climate effects of the flight need to be reported (see Table 2). Optionally, the take-off mass should be reported to allow e.g. for consistency checks. Highly sensitive airline data, like the exact fuel flow over time, however should be excluded from the reporting process, if possible.

Table 2: Possible EU ETS report of non-CO₂ effects per flights

Aircraft operator	Flight Date	Flight Number	Origin-Destination	AC & Eng. Type	Fuel Type	Fuel consumption [t]	CO ₂ [t]	CO ₂ e [t]

©DLR: Niklaß, Plohr, Dahlmann, Grawe

Any missing data for verification must either be requested by the agency from an independent data source, like the flown flight trajectory data from EUROCONTROL (see Section 2.2) or estimated itself via the CO₂e verification software, like the fuel flow along the trajectory (see Section 2.3).

2.2 Query and processing of flight plan data

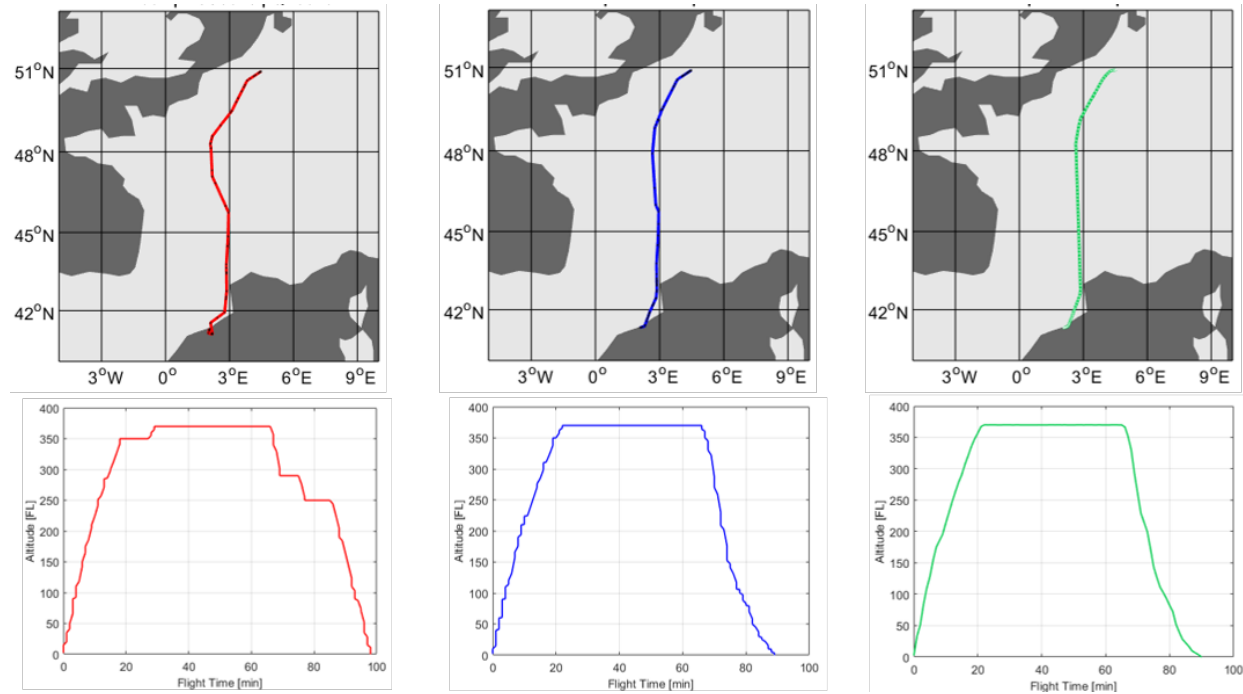
To query the flight profile from an independent data source like EUROCONTROL, the exact date, the flight number and (for consistency check) the aerodrome pair of the respective flight is needed (see Figure 4).

EUROCONTROL provides Operational Flight Plans (OFPs) via the Demand Data Repository (DDR2) based on airline-generated flight plan data. These OFPs are required for the Demand Capacity Balancing (DCB) function in the context of Air Traffic Flow and Capacity Management (ATFCM) in Europe. The computed 4-D-trajectories enable the determination of traffic demand for individual network elements, such as airspaces. Two types of flight plan data are available: model 1 data represents the last filed and saved flight plan after being finally modified, and model 3 data represents actual trajectories based on available position reports during flight execution, being processed post-operational. The DDR2 service from EUROCONTROL can be accessed online. Access needs to be granted, download volumes are limited according to account specifications.

In this study, model 3 data for 395 EAT flights and found a match in 389 cases (98.5%). were applied. For five flights (1.3%), the flight number provided by the airline was incomplete or different and could not be found in the DDR2 database. In one case (0.3%), the aircraft type specified by the airline did not match the model 3 data.

In general, a very good match between airline flight monitoring data and the EUROCONTROL's model 3 data was found (see Table 3: and blue and green lines in Figure 5).

Figure 5: Exemplary comparison of the last filed flight plan (model 1 data, red), the recorded flight path (model 3 data, blue) and the flight monitoring data of the airline (green) of a single flight



© DLR: Lau 2023 (source: EUROCONTROL, EAT)

For the 389 successful matches, the mean deviation in flight time and flight distance was less than 2.0%. Since model 3 data does not include taxiing time before take-off and after landing, a constant taxi time of 26 minutes was assumed for the calculation of the block time (= flight time + taxiing time) in accordance with the Landing Take Off (LTO) cycle defined by ICAO Annex 16. To estimate the block time of each flight, an average taxi speed of 30 kts was assumed according to DOC 9830 of ICAO (2004).

Table 3: Relative deviation (in %) between the airline's flight monitoring data and the DDR m3 flight profile data requested by EUROCONTROL

	Flight Time [Δ%]	Block Time [Δ%]	Flight Distance [Δ%]	Block Distance [Δ%]
Mean	-1.2%	+5.1%	-2.0%	-0.7%
Median	-1.2%	+3.4%	-0.7%	-0.6%

As shown in Table 3, airline monitoring data are in very good agreement with the model 3 data from EUROCONTROL. With a mean relative deviation in flight time and flight distance of -1.2% and -2.0%, respectively, model 3 data seem to be very well suited for the verification of location and weather dependent non-CO₂ effects. Since the distance flown at a certain altitude has a first-order effect on the climate impact of contrail induced cloudiness, a more precise flight profile data set significantly improves the CO₂e verification of CiC. With CO₂e(CiC) accounting on average more than 1/3 of total CO₂ equivalents, a big share of reported non-CO₂ effects can be verified with an appropriate precision, in case of a good match of the flight profiles.

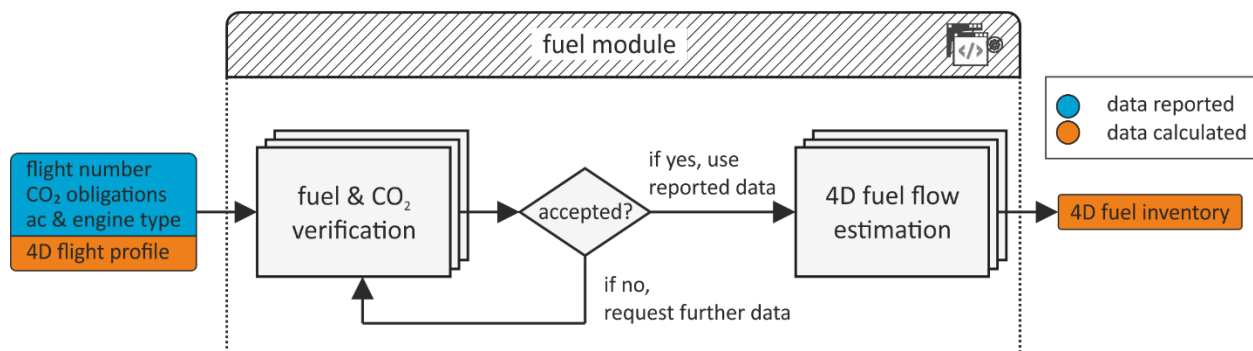
The roughly estimated taxi time of 26 minutes, however, clearly exceeds the monitored data of the airline. Taxi time is needed to estimate the fuel consumption and emissions during taxiing (see fuel burn module in Section 2.3). To improve taxi time estimation, statistical taxi times from European airports or individual airports (preferred) could be used.

Since the taxi distance corresponds better than the taxi time, the taxiing speed of 30 kts was also assumed to be too conservative for analyzed monitoring data. This assumption could be improved by better data from the literature (e.g. aircraft-specific taxi speed data). However, taxiing distance is not required for CO₂e validation and will not be used further.

2.3 Fuel burn module: Verification of the reported CO₂ and simplified Fuel Flow estimation

In addition to the existing MRV process, the fuel burn module is not only applied to the reported CO₂ (fuel) level, but also to estimate the fuel flow along the queried flight profile (see Figure 6) in order to generate a non-CO₂ emissions inventory (see emission module in Section 2.4 for the CO₂e calculation (see climate response module in Section 2.5).

Figure 6: Possible logic of the fuel burn module



©DLR: Niklaß 2023

If the difference between reported and estimated fuel (CO₂) is within a tolerance range, defined by the competent authority, we suggest using the reported data for fuel flow estimation to minimize subsequent differences. To find a proper level of detail, the fuel burn and fuel flow estimation has been performed in three different ways. We applied

1. aircraft specific regression formulas, like an extended version of EUROCONTROL's *Small Emitters Tool* (see Section 2.3.1),
2. aircraft and distance specific 3-D fuel profiles for various flight levels and load factors (see Section 2.3.2),

as well as higher fidelity models, like

3. detailed trajectory simulations taking wind effects into account (see Section 2.3.3).

Results are discussed in Section 3.

2.3.1 Application of aircraft specific regression formulas

The first method for estimating the 3-D Fuel Flow is based on EUROCONTROL's *Small Emitters Tool* (SET).

Under the current EU ETS, the use of the SET software for fuel burn calculation is permitted by the EC for small operators that emit less than 25,000 tons of CO₂ per year. The SET software

calculates the amount of fuel burnt (FB) [t] based on distance depended statistical regression formulas that are provided for most frequent aircraft types.

$$FB = f(\text{aircraft type, flight distance})$$

CO₂ emissions are estimated by a simplified version of the standard methodology for combustion emissions (European Commission, 2022):

$$CO_2 = FB \cdot EF$$

where EF is the CO₂ emission factor [t CO₂/t fuel], which is 3.15 for aircraft equipped with jet or turboprop engines.

For the 389 matched flights, the FB regression formulas have been applied 209 times for the aircraft type 'A306', 25 times for 'A332', 13 times for 'A333' and 163 for 'B752'. Table 4 shows the relative deviation (in %) between reported fuel data and fuel consumption estimated using SET regression formulas.

Table 4: Relative deviation (in %) between reported block fuel data and fuel consumption estimated with regression formulas

	All flights	A306	A332	A333	B752
Mean	+6.0%	+6.6%	-4.0%	-8.7%	+8.5%
Median	+6.8%	+6.8%	-4.9%	-9.7%	+9.4%
Max deviation	+28.7%	+26.2%	-16.2%	-14.1%	+28.7%

Despite unknown payload, unknown flight profile and unknown weather conditions (tailwind or headwind), fuel consumption was determined with an accuracy of about 6%. As the SET regression formulas are not designed for cargo aircraft, which are analyzed here, higher accuracy might be possible for passenger aircraft.

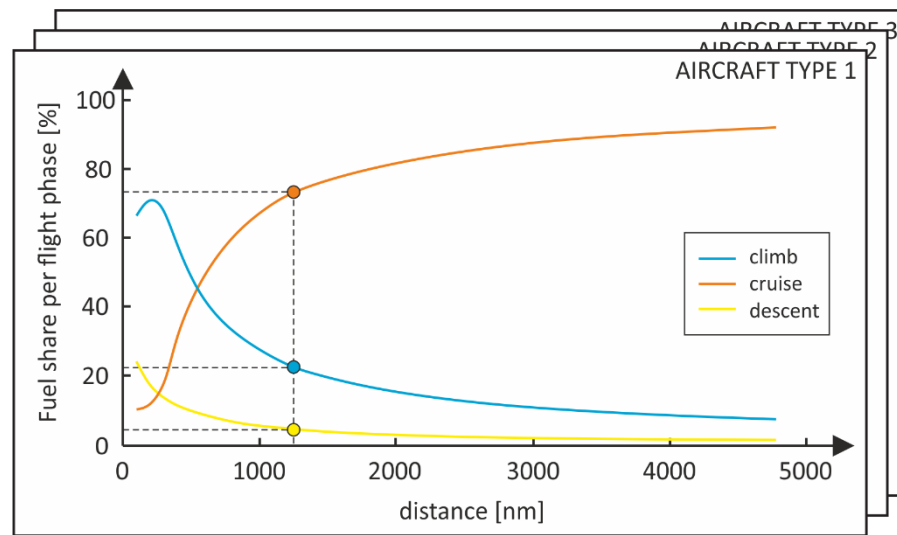
In all cases where the difference between reported and estimated fuel (CO₂) was within a tolerance range, the fuel burnt (FB_i) [t] was broken down into individual flight phases *i*. This was done by applying regression formulas, returning the aircraft specific fuel share (FS_i) [%] in the climb, cruise and descent phases as a function of the flight distance (*d*) (see Figure 7).

$$FB_i(d) = FS_i(d) \cdot (FB - FB_{\text{taxi}})$$

To generate the regression formulas, flight simulations were carried out with the Trajectory Calculation Module (TCM) (Lührs et al., 2014) for flight distances between 100 and 5000 nm under the assumption of fuel optimized flight altitudes, a load factor of 85% and International Standard Atmosphere (ISA) conditions. Aircraft performance of the four relevant aircraft types were obtained from EUROCONTROL's Base of aircraft data (BADA) 4.0 aircraft performance models (Nuic & Mouillet, 2012).

In the absence of statistics on the distance dependent taxiing fuel share, we approximated taxi fuel using the engine specific Idle Fuel Flow (FF_{idle}) [kg/s] from the ICAO's Engine Exhaust Emissions Database (EDB) and a constant taxiing time of 26 minutes as defined in the LTO cycle:

$$FB_{\text{taxi}} = FF_{\text{idle}} \cdot \text{time}_{\text{taxi}}$$

Figure 7: Relative fuel share per flight phase as a function of the flight distance

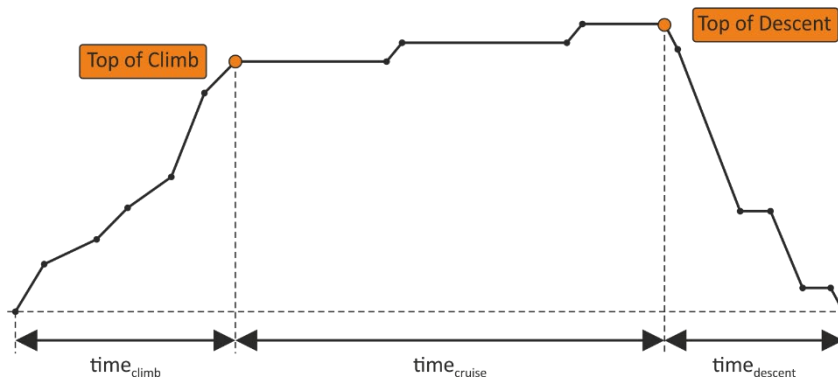
©DLR: Niklaß

In the shown example in Figure 7 of a 1250 nm flight, 73.5 % of fuel is burnt during cruise, 22 % during climb and around 4.5% during descent.

Based on the fuel burnt (FB_i) [kg] and the time_i [s] of the individual phases *i*, an averaged Fuel Flow (\overline{FF}_i) is estimated for the three flight phases climb, cruise, and descent

$$\overline{FF}_i = \frac{FB_i}{\text{time}_i}$$

Flight time of the individual phases are read from the 4-D flight profile, which are determined by the points Top of Climb (ToC, beginning of the cruise phase) and Top of Descent (ToD, beginning of the descent phase) (see Figure 8).

Figure 8: Identification of Top of Climb (ToC) and Top of Descent (ToD) to determine flight time during climb, cruise and descent

©DLR: Niklaß

Table 5 and Table 6 show the relative deviation (in %) between monitored (airline data) and estimated times, distances and fuel burn during climb, cruise and descent for all aircraft types.

Table 5: Relative deviation (in %) between monitored and estimated times and distances during climb, cruise and descent for all aircraft types

	Climb Phase		Cruise Phase		Descent Phase	
	Time	Dist.	Time	Dist.	Time	Dist.
Mean	+2.7%	+2.2%	-0.7%	-0.7%	-4.4%	-3.3%
Median	-1.9%	-2.1%	+0.6%	+0.9%	-5.2%	-3.9%
Max deviation	-66.5%	+74.3%	-73.6%	-73.6%	+132.3%	+179.3%

In general, the time and distance during climb, cruise and descent of all flights was estimated with an accuracy of more than 95%. For this reason, this simple approach seems appropriate. However, we also found very large deviations, in particular for the descent phase. Depending on whether a direct approach was possible or a holding pattern was necessary, the approach times varied greatly. In other cases, Top of Climb and Top of Descent was not identified with a necessary level of detail. Among others, this was caused by descent to lower flight levels within the cruise phase. More detailed elaboration of the identification logic might further reduce these errors. Otherwise, ToC and ToD could also be defined directly by the data provider.

Table 6: Relative deviation (in %) between monitored fuel burn and fuel burn estimated with regression formulas during climb, cruise and descent

	Climb Fuel	Cruise Fuel	Descent Fuel
Mean	+3.1%	+10.4%	-35.0%
Median	-0.2%	+9.3%	-36.8%
Max deviation	+102.6%	+109.3%	-77.2%

The distribution of fuel consumption worked well for the climb phase (agreement of 97% on average), was acceptable for the cruise phase (about 90%) and poor in the approach phase (about 65%). With a share of a few percent of the total fuel consumption (see yellow line in Figure 7), small absolute differences of descent fuel lead to significantly larger percentage deviations than in the other flight phases.

The main reasons identified was the significantly higher proportion of horizontal flight segments (step-descents, holding patterns) during the approach in the real flight data, and the Idle assumption when descending. To improve the accuracy of the fuel share functions, more level flight segments could be simulated during the approach or real flight data could be used for the generation of fuel share regression formulas (analogous to the SET fuel regression functions, preferred option). This would also reduce the fuel share of climb and cruise, which are currently overestimated by 3% and 10% respectively.

In future updates, fuel share regression formulas should also be provided for taxiing.

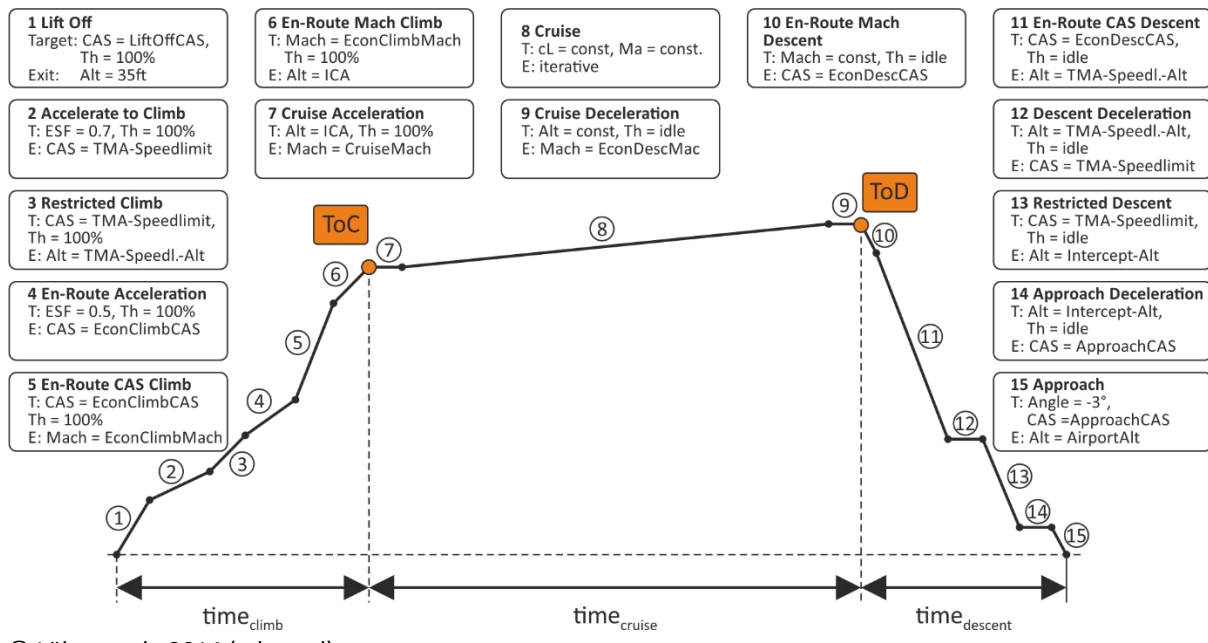
2.3.2 Application of aircraft and distance specific 3-D fuel profiles

In our second approach, the fuel flow approximation is based on interpolation of pre-computed data from similar flight profiles ("best guess"). For this purpose, a database of aircraft specific 3-D fuel profiles was generated for a variety of combinations of flight distances (d), flight levels

(FL) and load factors (LF). All data have been precalculated with TCM by applying BADA 4.2 aircraft performance models under ISA conditions.

Each fuel profile represents a typical flight mission for a specific set of d , LF, and FL and provides pre-calculated data of the relative flight time and position (altitude, distance), flight conditions (speed, lift, drag, thrust, mass) and FF at the beginning and end of every mission segments. Individual mission segments i are defined by specific Target and Exit conditions (see Figure 9). Target conditions have to be fulfilled during the given mission segment, e.g. constant flight speed. Exit conditions terminate the given mission segment, e.g. by reaching a certain altitude.

Figure 9: Vertical mission profile of reduced emission profiles (REP)



© Lührs et al., 2014 (adapted)

Most similar flight profiles are identified by the reported aircraft and engine type, the take-off mass (TOM, additional input from the airline), the flown flight distance, and the mean flight level during cruise (the latter two are retrieved from model 3 data):

$$FF_i = f(\text{aircraft type, TOM, flight distance, flight level, } i)$$

In order to project FF_i along the model 3 flight profile, we first calculate, analog to Section 2.3.1, the flight time during climb, cruise and descent based on ToC and ToD. In a second step, the individual segments i are identified by relative time share in climb (segments 1-6), cruise (7-9) and descent (10-15) of most similar flight profiles. Pre-computed FF_i are then interpolated for the actual mission and projected along the model 3 flight profile.

Burnt fuel flow is calculated from the fuel flow and the time:

$$FB_i = FF_i \cdot \text{time}_i$$

Fuel consumption during taxiing was calculated analog to Section 2.3.1.

Results are shown in Table 7 relative to the reported block fuel data:

Table 7: Relative deviation (in %) between reported block fuel data and fuel consumption estimated with 3-D fuel profiles and regression formulas (brackets)

	All flights	A306	A332	A333*	B752**
Mean	+3.6% (+6.0%)	+1.0% (+6.6%)	+2.3% (-4.0%)	+6.2% (-8.7%)	+7.9% (+8.5%)
Median	+2.7% (+6.8%)	+0.7% (+6.8%)	+2.3% (-4.9%)	+16.9% (-9.7%)	+8.5% (+9.4%)
Max deviation	+39.5% (+28.7%)	+39.5% (+26.2%)	+14.2% (-16.2%)	-34.7% (-14.1%)	+26.2% (+28.7%)

*A333 are equipped with a different engine type. Exact aircraft engine combination not available in BADA 4.2

**Airline uses two different engine types on the Boeing 752, but one combination is available in BADA 4.2

Based on 3-D fuel profiles, burnt fuel was estimated with an average accuracy of >96.5%, which is a slight improvement of around 2.5% over the regression formula approach. A particularly good agreement was achieved when BADA 4.2 aircraft performance models were available for the exact combination of aircraft and engine type (A306, A332). For Boeing 752, this was only the case for a sub-fleet, as only one of the two engine types used was available in BADA 4.2. For Airbus A333, we selected a different A333 BADA 4.2 model, as the equipped engine was not available.

The better the match between monitored flight profile and idealized fuel profile, the better the accuracy of estimated block fuel. Despite improved average accuracy, we see a significantly higher dependency of the 3-D fuel profiles on the model 3 data as well as ToC and ToD.

Whenever Top of Climb and Top of Descent were not identified correctly, we found high relative deviations of the estimated fuel burn of up to 40%. These are up to 10% larger than the maximum observed deviation of BF estimated with regression formulas that only take flight distance into account. More detailed elaboration of the ToC and ToD identification logic might further reduce these errors.

2.3.3 Detailed trajectory simulations taking wind effects into account

As a third option, detailed trajectory simulations were carried out with TCM. Besides the queried flight profile (model 3 data) and detailed aircraft performance data (BADA 4.2), the prevailing meteorological conditions are of significant relevance for detailed fuel and emission calculations. Weather data is acquired from the European Centre for Medium-Range Weather Forecast (ECMWF) and retrieved from the re-analysis v5 (ERA-5) dataset with a 0.5° horizontal resolution and highest available vertical resolution of 137 model levels (ECMWF 2022a,b). Using the positions (distances) and times of two consecutive model 3 data points (d_i, t_i), the speed over ground (GS_i) is determined and superposed with local wind data ($v_{w,i}$) to calculate the True Air Speed (TAS_i) and Mach number:

$$GS_i = \frac{d_i - d_{i-1}}{\text{time}_i - \text{time}_{i-1}}$$

$$TAS_i = GS_i + v_{w,i}$$

TAS_i and aircraft performance are used to calculate the lift and drag (D_i) of each point. Based on the total energy model, the necessary thrust (Th_i) is determined according to the following formula:

$$Th_i = D_i + \frac{dH_i}{dt} \cdot \frac{m_i \cdot g}{TAS_i} + m_i * \frac{dTAS_i}{dt}$$

where dH_i/dt is the rate of climb (retrieved from model 3 data), m_i the current aircraft mass (with $m_0 = \text{TOM}$; additional input from the airline), g the gravitational acceleration, and $dTAS_i/dt$ the acceleration (retrieved from model 3 and ERA-5 data).

In the last step, the aircraft specific FF_i is read out from the engine performance model as a function of Th_i and the prevailing temperature and pressure ratios.

The aircraft mass (m_{i+1}) at the next trajectory point ($i + 1$) is then calculated as follows:

$$m_{i+1} = m_i - BF_i$$

This calculation logic is iterated until the burnt fuel has been determined at each trajectory point:

$$BF = \sum_{i=1}^n FF_i \cdot \text{time}_i$$

In this study, these detailed simulations were conducted on the five days when the most frequent airline monitoring data were available (4 days in December 2021, 1 day in January 2022). A total of 52 flights were recalculated (28 Airbus A306 flights, 6 A332 flights, 5 A333 flights and 15 Boeing 757 flights). Results for the A306 and B752 flights are shown in Table 8.

Table 8: Relative deviation (in %) between reported block fuel data and fuel consumption estimated with detailed trajectory simulations and 3-D fuel profiles [square brackets]

	All flights	A306	B752
Mean	-3.2% [+3.6%]	-3.5% [+1.0%]	-2.6% [+7.9%]
Median	-3.2% [+2.7%]	-3.2% [+0.7%]	-3.2% [+8.5%]
Max deviation	-12.9% [+39.5%]	-12.5% [+39.5%]	-12.9% [+26.2%]

By performing detailed trajectory simulations with wind, the mean accuracy of the fuel estimation could be improved slightly further. Significantly greater improvements were found in the minimum and maximum deviation, which is about 20% lower than for 3-D fuel profiles. The

reason behind is that this methodology does not depend on the accuracy of identifying ToC and ToD. Instead, detailed calculations estimate BF_i separately for each trajectory point. However, inconsistent or imprecise time and location data in the model 3 datasets lead to strong fluctuations in the speed over ground (GS_i), and thus in TAS_i and acceleration ($dTAS_i/dt$). For few flights, these discontinuities caused multiple g accelerations between two points. The resulting errors in estimating fuels were so large and obvious that these values were not included in the statistics. One possibility to avoid these errors could be the use of smoothing functions (e.g. for ground speed).

2.4 Emission module: Evaluation of non-CO₂ emissions per flight

2.4.1 Evaluation of CO₂ and H₂O Emissions

Due to the high combustion efficiencies achieved in gas turbine engine combustors (greater than 99.9% for all high power operating conditions, not less than 98.8% at low power [Liu et al, 2017]), the emission indices of the main combustion products of hydrocarbon fuels, Carbon Dioxide (CO₂) and Water (H₂O), can be assumed to be constant for all relevant operating conditions (for local air quality assessments, more detailed models may be required for engine start-up and idle).

The ratio of CO₂ and H₂O emissions is then only dependent on the composition of the jet fuel. For a mean chemical sum formula for Jet A-1 kerosene of C₁₉H₂₃ (Rachner, 1998), the emission indices for CO₂ and H₂O for complete combustion are:

$$EI\ CO_2 = 3157.3\ g/kg\ Fuel$$

$$EI\ H_2O = 1237.2\ g/kg\ Fuel$$

These values can be applied to directly calculate CO₂ and H₂O emissions from the recorded fuel flow.

2.4.2 Evaluation of NO_x Emissions

In contrast, emissions of Nitrous Oxides (NO_x) are not a direct combustion product, but a by-product caused by oxidation of Nitrogen, contained in the air, under high combustion temperatures. As such, the NO_x production rate is strongly dependent on the combustion temperature and the residence time in the combustor (Lefebvre et al., 2010). Fortunately, in an existing gas turbine engine, all parameters affecting these values are interconnected. Therefore, it is possible to characterize an operating condition of a turbofan engine only by the ambient condition (given by air pressure, temperature and flight speed) and the fuel flow, which is the only parameter varied to control the engine thrust. As a consequence, a correlation exists between the flight condition, fuel flow and NO_x production. Several methodologies have been proposed to make use of this correlation to estimate the NO_x emission of an aircraft during flight, based on measured and certified sea level static engine emissions data as published in ICAO's EDB for each engine type in service.

For the purpose of this project the so-called Boeing Fuel Flow Method (BFFM) has been selected to estimate the NO_x emissions along the flight path of the individual flights considered. The method is described in detail in [Dubois and Paynter, 2007] and is recommended in ICAO's Environmental Technical Manual [ICAO, 2020] for the purpose of calculating NO_x emissions of individual flights. The required input data are engine fuel flow, ambient pressure and temperature as well as the flight Mach number, which can be calculated from ambient pressure, temperature and flight speed, if not available in the recorded flight data. Additionally, fuel flow

and EI NO_x data for the exact engine type from the EDB are needed. The methodology comprises a standardized step-by-step application procedure and is therefore well suited for automated application, e.g. as component of a software tool.

The methodology consists of the following 4 steps:

Step 1. Correct the current (measured/reported) Fuel Flow to ground reference conditions by

$$W_{ff} = \frac{W_f}{\delta_{amb}} \cdot \theta_{amb}^{3.8} \cdot e^{0.2 \cdot M^2} \quad \text{where } \theta_{amb} = \frac{T_{amb}}{288.15K} \text{ and } \delta_{amb} = \frac{p_{amb}}{101325Pa}$$

Step 2. Correct step 1 Fuel Flow for installation effects:

	Take-off	Climb-out	Approach	Idle
Thrust setting [% F ₀₀]	100%	85%	30%	7%
Correction factor r [-]	1.010	1.013	1.020	1.100

Step 3. Interpolate ground reference EI NO_x (REINO_x) in the EDB data by linear interpolation in log-log scale for the corrected Fuel Flow from step 2

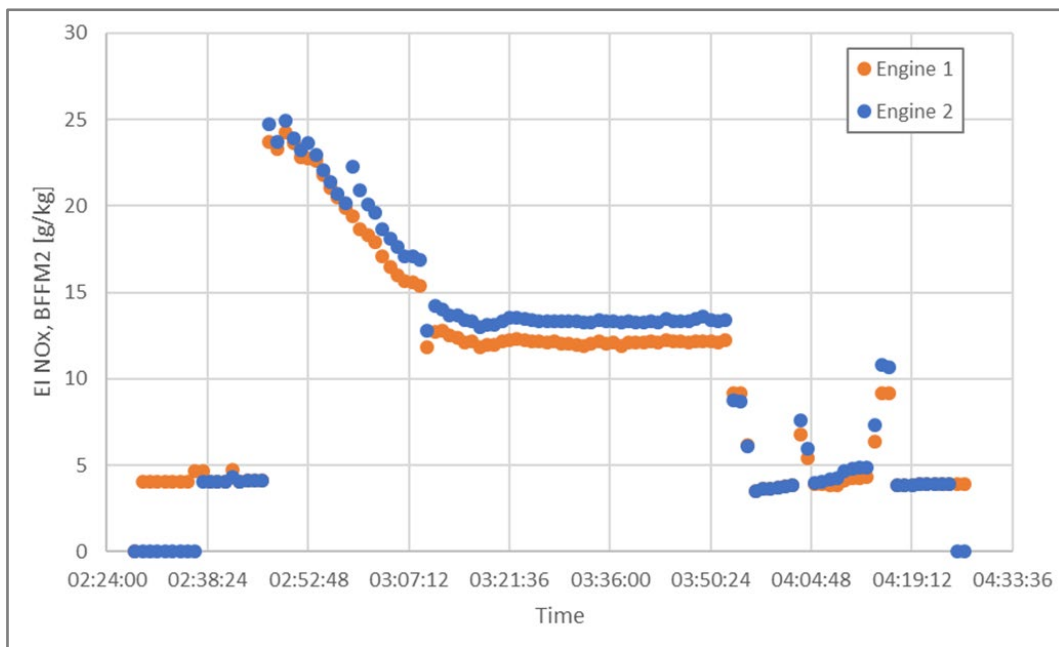
Step 4. Re-correct REINO_x for ambient conditions at the current flight condition by

$$EINO_x = REINO_x \cdot \sqrt{\frac{\delta_{amb}^{1.02}}{\theta_{amb}^{3.3}}} \cdot e^H$$

The term e^H in step 4 is a correction factor for ambient humidity. Since measured data of the current ambient humidity under flight conditions is mostly not available, usually a standardized, altitude-dependent correction is applied here.

An example of the application of this method to an EAT flight data recording is given in Figure 10:

Figure 10: Example of EI NO_x data calculated for a flight data recording with the Boeing Fuel Flow method



©DLR: Plohr, 2022

In this example, the initial low EI NO_x values are attributable to the Idle/Taxi operations before take-off. The Take-off run is easily identified by the sharp rise in EI NO_x, with it subsequently decreasing with the decreasing ambient pressure during the Climb phase. The Cruise phase is characterized by a lower, mainly constant EI NO_x value. The Descent phase shows mostly NO_x emissions in the Idle range (<5g/kg), sometimes interrupted by higher values supposedly caused by corrections to the descent path.

The noticeable difference between the two engines is probably caused by different maintenance conditions. During a longer period of operation, the performance of an aircraft engine will slowly degrade due to wear and abrasion, as well as deposition on the aerodynamic surfaces, resulting in lower efficiency and therefore more fuel required to provide the same thrust. The initial performance can usually be restored by a maintenance procedure.

2.4.3 Application of methodology for estimated Fuel Flow data

The approach described above has been applied to the different fuel burn and fuel flow estimation methods (see Section 2.3). Results for NO_x emissions are shown in Table 9:

Table 9: Relative deviation (in %) between NO_x emissions evaluated with monitored (Task1) and estimated (Task 2) Fuel Flow data. Results are shown for FF estimation based on regression formulas and detailed trajectory simulations (brackets)

	All flights	A306	A332*	A333*	B752
Mean	+6.8% (+0.7%)	+8.1% (-0.8%)	+11.3%	+2.7%	+4.6% (+8.5%)
Median	+4.0% (-2.6%)	+4.7% (-3.6%)	+5.6%	+1.8%	+3.3% (+9.4%)
Max deviation	+85.4% (+138.8%)	+85.4% (+138.8%)	+58.8%	+12.3%	+50.3% (+42.1%)

*Number of detailed trajectory simulations with A332 and A333 too small for evaluation.

On average, the levels of monitored and estimated NO_x emissions differ by +6.8% (regression formulas) and +0.7% (detailed trajectory simulation), respectively.

When using relative fuel share functions (regression approach), the burnt fuel ((BF_i)) were underestimated by -35% during descent and overestimated by +10% during cruise (see Figure 7 and Table 6). If, in addition, Top of Climb and Top of Descent have not been hit correctly in this approach, there was also a mismatch of estimated time in mode ($time_i$), which further increased the deviation of monitored and estimated fuel flow ($FF_i = BF_i/time_i$). Since FF_i is the main input for the emission module, this has a direct impact on accuracy of the level and spatial distribution of NO_x emissions. In extreme cases, we identified a maximum deviation of NO_x descent emissions of up to 330%. In order to reduce these consequential errors, an update of fuel share regression formulas with real flight data as well as a more detailed elaboration of the ToC and ToD identification logic seems to be absolutely necessary.

As an alternative, NO_x emission inventories can also be generated with sufficient accuracy by applying detailed trajectory simulations that also takes wind data into account. However, these simulations are much more complex and therefore more difficult to automate.

2.4.4 Uncertainties of NO_x prediction

A comparison of several NO_x correlation methods and an estimate of their accuracy, when compared with (undisclosed) OEM data, was provided in the final technical report of the EC-project NEPAir (Norman et al., 2003). In this report, an accuracy of $\pm 10\%$ is given for NO_x predictions by the BFFM for conventional RQL combustors. Methods with better accuracy are described in the project, but those require knowledge of internal engine temperatures and pressures which are usually only available to the engine OEM.

A procedure for application of the BFFM to advanced low NO_x combustors, featuring staged, lean-burn technology is under development by ICAO CAEP's Working Group 3. Due to additional (usually unknown) parameters determining the combustion staging, it is expected that this method will be unable to achieve the same accuracy as for conventional combustors.

Further sources of uncertainties can arise from the required reference data for application of the BFFM. Although emissions and fuel flow data for every engine in service is available through the ICAO EDB, the engine designation is not always unambiguous. There are engine variants with the same engine designation in the database featuring different combustion systems with sometimes very different NO_x emission behaviour. If an airline doesn't know the exact UID of the ICAO EDB entry of their engines, it is not possible to accurately estimate the NO_x emissions of a flight. In this case it is recommended to use averaged EI NO_x data from all engine variants with the same designation. While this would still result in higher uncertainties for an individual flight, the uncertainties will likely balance out for a larger number of flights with several aircraft propelled by the engine types in question.

2.5 Climate-response module: Evaluation of CO₂ equivalents per flight

To calculate the CO₂e for the provided routes we use the climate response model *AirClim* (Dahlmann et al., 2016; Grewe & Stenke, 2008). *AirClim* is a non-linear climate response model, which combines aircraft emission data (longitude, latitude and altitude) with a set of previously calculated atmospheric responses to calculate the temporal development of the global near-surface temperature change.

For deriving the atmospheric responses for H₂O and NO_x-induced changes in O₃ and CH₄, 85 steady-state simulations for the year 2000 were performed with the DLR climate-chemistry

model E39/CA, prescribing normalized emissions of NO_x and H₂O at various atmospheric regions (Fichter, 2009). For the impact of contrail induced cloudiness (CiC) we use atmospheric and climate responses considering local probability of fulfilling the Schmidt-Appleman Criterion (SAC) as well as ice supersaturated regions, which were obtained from simulations with ECHAM4-CCMod from Burkhardt and Kärcher (2009, 2011).

Note that we follow a climatological approach in the calculation of the climate impact and the calculated values for the climate impact represent a mean over all weather situations averaging over individual spatially and temporally resolved responses.

AirClim is a very efficient response tool and is able to calculate the climate impact of a single route in less than one minute on a standard PC. Therefore, it is possible to automate the CO₂e calculations.

As a metric we use here the ATR100, which is the average near surface temperature response over 100 years. As an emission development we assume increasing emissions in the future according to Grewe et al., 2021. One could also use pulse emissions (emissions only in one year) to calculate the CO₂e, but here we use increasing emissions to compare the results to work package 3. Note, that the level of total CO₂e values strongly depends on the level of the CO₂ reference and therefore on the emission development. Since EU ETS is designed to estimate the climate impact of present and future flights, CO₂e values do here not include emissions of historic aviation. As the climate impact of CO₂ is more affected by the historical emission than short lived non-CO₂ effects, the share of non-CO₂ effects (here about 75%) is higher than the known factor from the literature for non-CO₂ effects of 2-3, which is based on the total CO₂ level from preindustrial times (e.g. from 1940 to 2018 for Lee et al., 2021). CiC contributes about 51.4% to total CO₂e values. Water vapour emissions account for 2.7% and nitrogen oxides for about 22.4%. *AirClim* is a DLR tool without free access at the moment. But an open Version of *AirClim* will be developed which should be available by end of 2024. This version will be designed for research purpose with a lot of parameters which can be freely chosen. For MRV purposes we assume that a kind of Blackbox version would be suitable, with fixed parameters and exactly defined input and output. Such a version could be developed quite fast.

Beside *AirClim*, other climate-response models are available that consider the temporal development of the climate impact (Lim et al., 2006) or the altitude dependency (Köhler et al., 2008; Rädel and Shine, 2008). For location-dependent CO₂ equivalents, the climate response simulation however must at least take latitude and altitude dependency into account.

In this section the climate impact in terms of CO₂e for all routes from estimated emissions (Task 2) are compared to the climate impact of monitored emissions (Task 1). The relative deviation between reported and estimated CO₂e values are shown in Table 10.

Table 10: Relative deviation (in %) between CO₂e emissions evaluated with monitored (Task 1) and estimated (Task 2) Fuel Flow data. Results are shown for FF estimation based on regression formulas and detailed trajectory simulations (brackets)

	Total	H ₂ O	CiC	NO _x
Mean	+5.2% (-3.6%)	+14.8% (-0.6%)	-1.7% (-1.5%)	59.1% (-1.1%)
Median	+4.2% (-3.5%)	+14.1% (+1.5%)	+0.1% (-0.3%)	24.7% (-29.3%)
Max deviation	-105.9% (-16.9%)	+108.0% (-21.2%)	-68.7% (-11.2%)	549.8% (296.5%)

*Number of detailed trajectory simulations with A332 and A333 too small for evaluation.

On average, estimated and reported CO₂e(total) values differ by +5.2% (regression formulas) and -3.60% (detailed trajectory simulation), respectively. Detailed trajectory simulation led to a more accurate CO₂e estimation for all considered climate agents.

With an average error of about 2%, the climate impact of CiC was estimated particularly well. Since the queried flight profile data from EUROCONTROL matches very well with the monitored data of the airline, the distance flown at a certain altitude (first-order effect on the climate impact of contrail induced cloudiness) is almost identical in both data sets. Model 3 data therefore seems to be very well suited for verifying CO₂e(CiC). Any differences in CO₂e(CiC) between the two fuel burn approaches can be attributed mainly to varying sample size.

Differences of CO₂e(H₂O) are mainly caused by an inaccurate estimate of the 4-D fuel flow. Since the regression functions overestimated the fuel consumption during cruise by 10.4% (see Table 6), more H₂O emissions have been released at high altitudes. In higher altitudes the impact of H₂O emissions is larger as the lifetime increases.

CO₂e(NO_x) show by far the highest inaccuracy (median deviation of about 25%), especially for regression functions where consequential errors are particular high. If burnt fuel (BF_i) and time in mode (time_i) are not hit correctly in this approach, the estimated average fuel flow of the three main phases will deviate strongly from monitored FF values (FF_i = BF_i/time_i). This results to an incorrect level and distribution of NO_x emissions and thus to an incorrect climate assessment, which is off by several orders of magnitude in individual cases. In order to reduce these consequential errors, an update of fuel share regression formulas with real flight data as well as a more detailed elaboration of the ToC and ToD identification logic seems to be absolutely necessary.

By applying detailed trajectory simulations that also takes wind data into account, CO₂e(NO_x) values have been estimated with an averaged accuracy of -3.7%. However, strong discrepancies were still found in individual cases. Since this methodology is significantly more complex, it is also more difficult to automate.

3 Comparison of CO2e with results of DLR simplified CO2e estimator (Task 3)

In Tasks 1–3 of the project, CO₂ equivalents have been calculated in three different ways, that differ mainly in the availability of data. The CO₂e estimation of Task 1 is based on flight monitoring data that is provided directly by the aircraft operator (see Plohr et al., 2023). In this case, 4-D emission inventories have been computed based on fuel flow records. Task 2 addresses the verification of reported CO₂e without any information of the fuel flow along the 4-D flight profile (see Section 1-2 of current report). A simplified CO₂e estimation methodology has been developed in Task 3, which only use the information of city pairs and aircraft seat category (see Dahlmann et al., 2023). A comparison of the CO₂e values calculated in Task 1 and 3 is carried out in the following subsections 3.1 and 3.2.

For this study, the CO₂e values for all analyzed EAT city pair connections (Task 1) were additionally calculated with the DLR simplified CO₂e estimator. The aircraft category, which was used for the different aircraft, is listed in Table 11.

Table 11: Assignment of aircraft data to seat categories

	A306	A332	A333	B752
Typical number of seats	250-350	253-404	295-440	200-239
Assigned seat category	252-300	301-600	301-600	202-251

3.1 Emissions

On average the reported fuel consumption and the fuel consumption calculated with the simplified CO₂e estimator differ by about +17 % with a spread between -19 and +59 % (Table 12). Considering that there was already a scatter of approx. 20% in the EAT fuel monitoring data for individual routes and individual cargo aircraft (see Figure 4 in Plohr et al., 2023), the fuel estimates provided in Task 3 for a representing commercial aircraft of similar size agree reasonably well. The mean relative difference of NO_x emissions is with +5 % lower than for fuel consumption, but with a larger spread between -37 and +70 %. The difference in flown distance is in median zero with a spread between -14 and +16 %.

Table 12: Relative deviation (in %) between fuel, NO_x emissions and flown distances evaluated with monitored (Task 1) trajectories and the DLR simplified CO₂e estimator.

	fuel consumption	NO_x emissions	flown distances
2.5% Percentile	-19%	-37%	-14%
25% Percentile	-3%	-20%	-5%
Median	17%	5%	0%
75% Percentile	33%	37%	6%
97.5% Percentile	59%	70%	16%

3.2 Climate impact

On average the total CO2e calculated with the DLR simplified CO2e estimator (Task 3) are about 42% larger than the reported total CO2e (Task 1) with a spread between -8 % and +128 % (see Table 13). In accordance to the difference in fuel consumption the CO2 climate impact, calculated with the DLR simplified CO2e estimator, is about 18 % larger than the reported CO₂ impact.

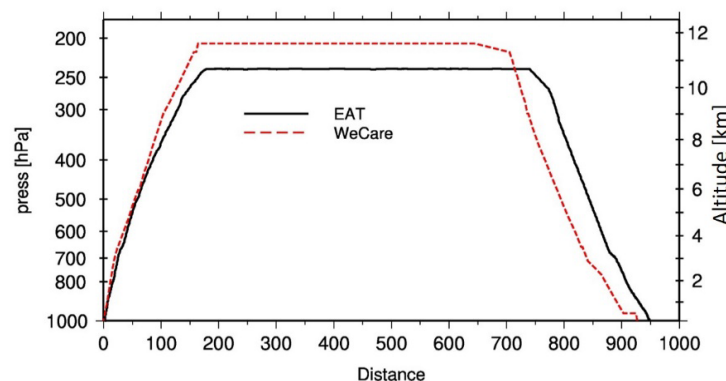
The other species show a larger difference than the difference in emissions would suggest. The largest difference can be seen for CO2e(H₂O). On median the DLR simplified CO2e estimator calculates a 138 % larger impact of H₂O compared to the reported H₂O impact. In extreme cases the difference is up to 1162 %. Nevertheless, this large difference has only a minor impact on the total climate impact as the contribution of H₂O to the total aviation climate impact is very small. For the climate impact of NO_x we investigated a median overestimation of 48 % with a spread between -65 % and 197 %. For the climate impact of CiC the median is overestimated by 672 % with a spread between -65 % and +4943 %.

The reasons for the differences are on the one hand side the differences in the total emissions and on the other hand differences in the emission distribution. For a detailed investigation for the large differences, we took a closer look at the route ATH (Athen, Greece) to LCA (Lanarca, Cyprus). For this route, detailed AirClim simulation have been conducted both for EAT flights (Task 1) and the WeCare flight database (Task 3), which was used for creating CO2e regression formulas. This allows us to examine whether the differences are caused by the different flight profiles (comparison of EAT and WeCare trajectories with AirClim) or by the regression formulas itself (comparing WeCare database and DLR simplified CO2e estimator results).

Table 13: Relative deviation (in %) between CO2e emissions evaluated with monitored (Task) Fuel Flow data and the simplified CO2e estimator.

	Tot	CO ₂	H ₂ O	NO _x	CiC
2.5%Perzentile	-8%	-18%	-5%	-4%	-65%
25%Perzentile	27%	-2%	47%	24%	122%
Median	42%	18%	138%	44%	672%
75%Perzentile	63%	34%	266%	74%	839%
97.5%Perzentile	128%	61%	1162%	197%	4943%

Figure 11: Altitude profile for the route ATH-LCA



The direct comparison of *AirClim* results of the two trajectories (EAT and WeCare, Table 14), shows that WeCare clearly overestimates the effect of H₂O and NO_x (81% and 6%), despite underestimated fuel consumption (-14%) and NO_x emissions (-16%). This difference is mainly caused by different altitude profiles of the two trajectories (see Figure 11: ). Since WeCare reaches higher altitudes on cruise flights (206 instead of 240 hPa), the climate impact of H₂O and NO_x are higher (both effects strongly increase with altitude in this region). When comparing the EAT altitude profile with WeCare flights of comparable distances, a similar offset in cruise altitude was found, indicating an overestimation of H₂O and NO_x for all flights. In addition to these differences the DLR CO₂e estimator fit the results from WeCare with an error of 5% and 17 % for NO_x and H₂O, respectively (Table 15).

Table 14: CO₂e calculated with reported trajectories (Task 1, EAT) and WeCare trajectories (used for regression formulas) and relative deviation of WeCare to EAT.

	Total	CO ₂	H ₂ O	NO _x	CiC	fuel	NO _x	dist
EAT	48067	19833	1379	22325	4530	6367	102	954
WeCare	46415	17032	2499	23687	3198	5468	86	930
Relative deviation	-3%	-14%	81%	6%	-29%	-14%	-16%	-2%

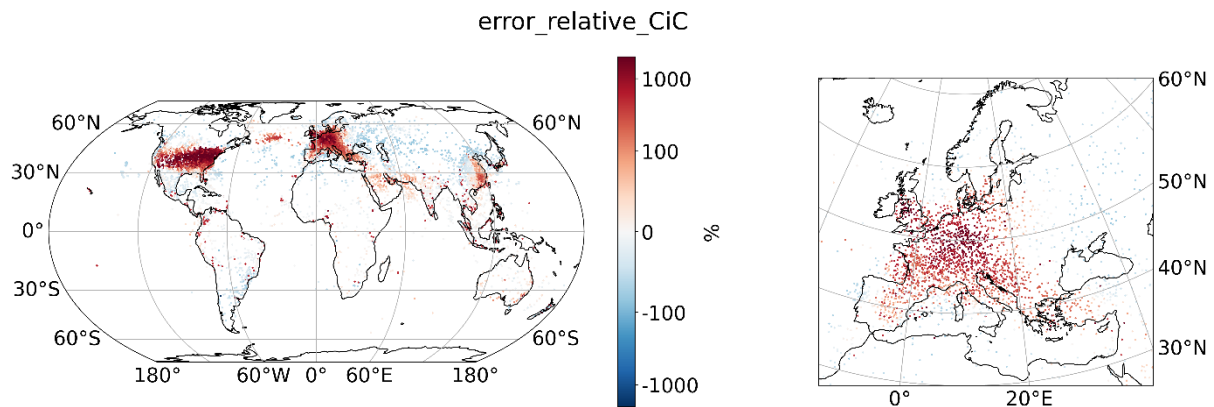
Table 15: CO₂e calculated with WeCare trajectories and results from DLR CO₂ estimator normalized to WeCare fuel consumption and relative deviation of DLR CO₂ estimator and WeCare.

	Total	CO ₂	H ₂ O	NO _x	CiC
WeCare	46415	17032	2499	23687	3198
DLR CO ₂ e estimator normalized	49224	17218	2934	24826	4246
Relative deviation	6%	1%	17%	5%	33%

In addition to different altitude distributions, the strong overestimation of the climate impact of CiC is caused by the modeling of saturation effects. In this study, *AirClim* simulations have been conducted based on emission inventories composed by individual flights (input) and background emissions (assumption). In regions with particular high air traffic (high background emissions) saturation effects occur. An additional emission therefore has a smaller effect than in regions with low air traffic density. This effect is accounted in the same way for Task 1 and the Task 3 WeCare flight database used for creating CO₂e regression functions. But, however, since the CO₂e regressions for CiC have been modeled only as function of mean latitude and distance, regions with high (Europe, USA) and low background emissions (Russia, Pacific) have been averaged. The resulting relative error of CO₂e(CiC) visualized in Figure 12 for all routes of the WeCare flight database at their mean longitude and latitude. There you can see that in Europe and the USA in particular, i.e. in areas with a high volume of air traffic, the climate impact is sometimes significantly overestimated. Since our comparison is based almost

exclusively on intra-European flights, saturation effects were significantly underestimated in Task 3 in contrast to Task 1.

Figure 12: Relative deviation of the CO₂e calculated with the DLR simplified CO₂e estimator and AirClim calculations (logarithmic scale)



To avoid this overestimation in a future version of DLR's simplified CO₂e estimator, an additional dependence on the mean longitude could be considered. Alternatively, an attempt could be made not to calculate the effect for additional emissions (perturbation) but for the contribution to the overall effect of the emissions (tagging).

4 Summary

In the present report we took over the perspective of a competent authority and analyzed all necessary tasks for verifying location-dependent CO₂ equivalents reported for the EU ETS (Input from work package 1, EU ETS report). Our demonstration is based on flight monitoring data from 449 mainly intra-European flights of four different aircraft types (A300, A330-200, A330-300, B757), which were provided by the European Air Transportation Leipzig (EAT) cargo airline.

For reducing the MRV effort of non-CO₂ effects in EU ETS, we suggest to use a standardized CO₂e software, which might be provided or approved by the European commission (EC) for airlines (monitoring and reporting) as well as verifiers and authorities (verification and assessment). In this regard, the current EU ETS system serves as a blueprint, for which EUROCONTROL provides a web application called ETS Support Facility (ETS SF) for operators and agencies (EUROCONTROL, 2022). For the verification of location-dependent CO₂ equivalents, the standardized CO₂e software should perform following steps:

1. the query and processing of flight profile data from an independent data source like EUROCONTROL,
2. the verification of the reported CO₂ (fuel burn) and a simplified estimate of fuel flow along the recorded flight path,
3. the computation of emission inventories for CO₂, H₂O and NO_x along the flight path, and
4. the CO₂e estimation of the flight for H₂O, NO_x, CiC under consideration of uncertainties (e.g. 5% percentile, 50% percentile, 95% percentile) for different climate indicators (e.g. ATR, GWP) and time horizons (e.g. 20, 50, 100 years).

Following the physical-based modules, the EU decision is implemented in a policy-based module in order to set the level of CO₂e obligations (e.g., depending on the confidence levels of each climate agent):

5. Allocation of CO₂e obligations (policy-based module, not part of this project)

Analogous to the CO₂ monitoring in EU ETS and under CORSIA, different computation methods can be made available for the three physical-based modules (fuel burn module, emission module and climate response module). The selection of the calculation methods used by an individual aircraft operator should be specified in the airline specific Emission Monitoring Plan (EMP) and submitted to the competent authority for approval.

To better understand the impact of uncertainties on the calculation of non-CO₂ effects and thereby on the potential of setting wrong incentives, risk assessments are required for selected climate agents. First, the climate mitigation potentials of specific strategies have to be verified. Second, reported CO₂e values have to represent estimated climate impact of aviation on average. This requires a solid data base, including flight information, fuel consumption as well as CO₂ equivalents from numerous flights. Necessary data could be collected in the pilot non-CO₂ MRV scheme of the EU ETS starting in 2025, in which non-CO₂ effects are already monitored and reported, but are not yet subject to monetary internalization.

In order to obtain the 4-D flight profile from an independent data source, we applied model 3 data from EUROCONTROL, which correlates very well with the recorded airline flight profiles. With a mean relative deviation in flight time and flight distance of -1.2% and -2.0%, respectively, model 3 data seem to be very well suited for the verification of location (and weather) dependent non-CO₂ effects.

For the verification of the reported CO₂ and simplified fuel flow estimation (fuel burn module), we applied simple regression formulas (extended version of EUROCONTROL's Small Emitters Tool) as well as 3-D fuel profiles and detailed trajectory simulations that also take into account wind effects. The higher the level of detail, the higher the accuracy of the estimated burnt fuel and estimated fuel flow and the lower the susceptibility to consequential errors. Since the complexity increases at the same time, automation becomes more difficult.

For the automated calculation of NO_x emissions, the Boeing Fuel Flow Method (BFFM) was implemented into a software tool which applies this method on the basis of engine-specific, certified sea level static emissions data from the ICAO EDB for every data point in the estimated fuel flow profile of each flight. Subsequently, the estimated emission inventories were manually provided to the CO₂e calculations.

The evaluation of CO₂e per flight has been carried out with the DLR's climate response model *AirClim*. However, there is no public version of *AirClim* available at the moment but an open source version is currently under development, which should be available by end of 2024. The open *AirClim* version is developed for research purposes with many parameters that can be freely changed. For MRV purpose, a user friendly "black box" version would be more suitable, with fixed parameters and well-defined input and output parameters. Such an *AirClim* version could be developed in a shorter time. Beside *AirClim*, other climate-response models are available that consider the temporal development of the climate impact or the altitude dependency. For location-dependent CO₂ equivalents, the climate response simulation however must at least take latitude and altitude dependency into account.

On average, estimated and reported CO₂e(total) values differ by +5.2% (regression formulas) and -3.6% (detailed trajectory simulation), respectively. Detailed trajectory simulation led to a more accurate CO₂e estimation for all considered climate agents. With an average error of about 2%, the climate impact of CiC was estimated particularly well. CO₂e(NO_x) show by far the highest inaccuracy (median deviation of about 25%), especially for regression functions where consequential errors are particular high. In order to reduce these consequential errors of simple regression formulas, fuel share regression formula should be based on real flight. More detailed elaboration of the top of climb (ToC) and top of descent (ToD) identification logic might further reduce these errors.

The comparison between reported CO₂ equivalents and the CO₂ equivalents calculated with the DLR CO₂e estimator differ by a median of 42%. The effect of CO₂ is overestimated by about 18% due to the overestimated emissions. In addition, the effect of H₂O and NO_x is overestimated in median by 138 and 44%, respectively, since the EAT flights fly at lower altitudes than assumed for the regression. The biggest difference is caused by the contrail cirrus. The reason for the strong overestimation of around 670% is the fact that the flights examined mainly take place over Europe and AirClim calculates a low impact here due to saturation effects, which are not yet reflected accordingly in the regression formulas of the DLR tool.

For the automatic verification of CO₂e of individual flights, it is necessary to develop a unified software that contains all steps with automatic processing and transfer of data. This also requires the definition of a tolerance range for reported CO₂ equivalence values by the competent authority.

5 List of references

Burkhardt, U. und Kärcher, B. (2009), 'Process-based simulation of contrail cirrus in a global climate model', *J. Geophys. Res.* 114(D13), D16201.

Burkhardt, U. and Kärcher, B. (2011): Global radiative forcing from contrail cirrus. *Nat. Clim. Chang.*, 1, 54–58

Cames, M., Graichen, J., Siemons, A., Cook, V. (2015): Emission Reduction Targets for International Aviation and Shipping, Policy Department A for the Committee on Environment, Public Health and Food Safety (ENVI). IP/A/ENVI/2015-11.

Dahlmann, K., Koch, A., Linke, F., Lührs, B., Grewe, V., Otten, T., Seider, D., Gollnick, V. and Schumann, U. (2016): Climate-Compatible Air Transport System—Climate Impact Mitigation Potential for Actual and Future Aircraft. *Aerospace*, 3, 38.

Dahlmann, K., Thor, R., Grewe, V., Niklaß, M., Linke, F. (2024): Software for a simplified estimation of CO₂ equivalents of individual flights, *Climate Change: 27/2024*, Umweltbundesamt. FKZ: 3720-42-502-0.

Dubois D., Paynter, G. C. (2007): „Fuel Flow Method 2“ for Estimating Aircraft Engine Emissions, SAE Technical Paper 2006-01-1987, SAE international

European Centre for Medium-Range Weather Forecasts (2022a): Atmospheric Reanalysis v5 (ERA5)
<https://www.ecmwf.int/en/forecasts/dataset/ecmwf-reanalysis-v5>, last accessed May 10, 2022

European Centre for Medium-Range Weather Forecasts (2022b): L137 model level definition
<https://confluence.ecmwf.int/display/UDOC/L137+model+level+definitions>, last accessed June 10, 2022

European Commission (2022): EU ETS Monitoring and Reporting – Quick guide for aircraft operators Updated for EU ETS Phase 4 – Version of 1 March 2022, https://ec.europa.eu/clima/system/files/2022-03/quick_guide_ao_en.pdf (accessed on 26 August 2022)

European Parliament (2022): Amendments adopted by the European Parliament on 8 June 2022 on the proposal for a directive of the European Parliament and of the Council amending Directive 2003/87/EC as regards aviation's contribution to the Union's economy-wide emission reduction target and appropriately implementing a global market-based measure (COM(2021)0552 – C9-0319/2021 – 2021/0207(COD)), https://www.europarl.europa.eu/doceo/document/TA-9-2022-0230_EN.pdf, 2022

EUROCONTROL (2022): Emissions Trading System Support Facility,
<https://www.eurocontrol.int/service/emissions-trading-system-support> (accessed on 26 August 2022)

Faber, J., Greenwood, D., Lee, D., Mann, M., de Leon, P. M., Nelissen, D., Owen, B., Ralph, M., Tilston, J., van Velzen, A., & van de Vreede, G. (2008). Lower NO_x at higher altitudes. Policies to reduce the climate impact of aviation NO_x emission. CE Delft.

Fichter, C. (2009). Climate Impact of Air Traffic Emissions in Dependency of the Emission Location and Altitude. Dissertation Manchester Metropolitan University, Manchester, UK

Grewe, V. and Stenke, A. (2008): AirClim: An efficient climate impact assessment tool. *Atmos. Chem. Phys.*, 8, 4621–4639

ICAO (2013): International Civil Aviation Organization, Global Air Transport Outlook to 2030 and trends to 2040. Montreal. Circular 333, AT/190.

ICAO (2004) DOC 9830: Advanced Surface Movement Guidance and Control Systems (A-SMGCS) Manual

Lee, D.S., Fahey, D.W., Skowron, A., Allen, M.R., Burkhardt, U., Chen, Q., Doherty, S.J., Freeman, S., Forster, P.M., Fuglestvedt, J., Gettelman, A., De León, R.R., Lim, L.L., Lund, M.T., Millar, R.J., Owen, B., Penner, J.E., Pitari, G., Prather, M.J., Sausen, R., Wilcox, L.J. (2021): The contribution of global aviation to anthropogenic

climate forcing for 2000 to 2018, Atmospheric Environment, Volume 244, 2021, 117834, ISSN 1352-2310, <https://doi.org/10.1016/j.atmosenv.2020.117834>.

Lefebvre A. H., Ballal, D. R. (2010): Gas Turbine Combustion, 3rd edition, ISBN 978-1-4200-8605-8, CRC press, Boca Raton, FL

Matthes, S.; Lim, L.; Burkhardt, U.; Dahlmann, K.; Dietmüller, S.; Grewe, V.; Haslerud, A.S.; Hendricks, J.; Owen, B.; Pitari, G.; Righi, M.; Skowron (2021): A. Mitigation of Non-CO₂ Aviation's Climate Impact by Changing Cruise Altitudes. Aerospace 2021, 8, 36. <https://doi.org/10.3390/aerospace8020036>

Niklaß, M., Dahlmann, K., Grewe, V., Maertens, S., Plohr, H., Scheelhaase, M., Schwieger, J., Brodmann, U., Kurzböck, C., Repmann, M., Schweizer, N., & von Unger, M. (2020). Integration of non-CO₂ effects of aviation in the EU ETS and under CORSIA. Climate Change: 20/2020, Umweltbundesamt. FKZ:3717-42-509-0.

Niklaß, M., Linke, F., Dahlmann, K., Grewe, V., Matthes, S., Plohr, M., Maertens, S., Wozny, F., Scheelhaase, J. (2024): Decision parameters of an MRV scheme for integrating non-CO₂ aviation effects into EU ETS, Climate Change: 30/2024, Umweltbundesamt. FKZ: 3720-42-502-0.

Plohr, M., Dahlmann, K., Niklaß, M. (2024): Testing of a monitoring and reporting scheme for integrating non-CO₂ aviation effects into EU ETS, Climate Change: 25/2024, Umweltbundesamt. FKZ: 3720-42-502-0.

Norman, P., Lister, D., Lecht, M., Madden, P., Park, K., Penanhoat, O., Plaisance, C., Renger, K. (2003): NEPAir Final Technical Report, EC Contract Number G4RD-CT-2000-00182

Nuic, A., & Mouillet, V. (2012). User manual for the base of aircraft data (BADA) family 4 (ECC Technical/Scientific Report No. 12/11/22-58).

Rachner, M. (1998): Die Stoffeigenschaften von Kerosin Jet A-1, DLR-Mitteilung 98-01, Institut für Antriebstechnik, DLR, Köln

Scheelhaase, J., Dahlmann, K., Jung, M., Keimel, H., Nieße, H., Sausen, R., Schaefer, M., & Wolters, F. (2016). How to best address aviation's full climate impact from an economic policy point of view? – Main results from AviClim research project. Transportation Research Part D: Transport and Environment, 45(1), 112–125. <https://doi.org/10.1016/j.trd.2015.09.002>.